Modelling, analysis, and optimisation of the rear axle of cereal combine harvester under real loads using finite elements method

Azam Rezaei, Hassan Masoudi, Hassan Zaki Dizaji, Mohamad Esmail Khorasani Ferdavani

Department of Biosystems Engineering, Faculty of Agriculture, Shahid Chamran University of Ahvaz, Iran

Abstract

Cereals combine harvester is one of the agricultural machines that work under challenging conditions, and different forces are applied to its parts. This study aimed to analyse static and dynamic loads on the rear axle of the JD955 combine harvester to optimise it. First, real loads on the axle were measured by a special electronic system in stationary and moving modes on roads and farms with various forward speeds. Then, a geometric model of the axle was designed in the CATIA software. Finally, the ANSYS Workbench software performed static, harmonic, transient, and dynamic analyses using the finite element method. The mean of maximum loads on the axle in stopped mode, asphalt road, dirt road, and inside the farm (while moving parallel and perpendicular to the farrows and turning in farm end) were equal to 15.067, 18.830, 49.167, 21.428, 27.07 and 27.857 KN, respectively. There was a relatively linear relationship between the axle load and deformation. At the maximum load of 49.167 KN, the maximum von Mises stresses of 1200, 85.848, 21.392, and 1.754e-14 MPa were obtained in static, transient, dynamic, and harmonic analyses, respectively. Since structural errors in the axle were numerically close to zero, the calculated stress values had good accuracy. The axle fatigue life for most loads was equal to the ideal value of 10^6 cycles. The least fatigue safety factor was obtained from 0.072 to 0.745 in static analysis and from 0.174 to 1.029 in linear transient analysis. According to the analysis results, it was necessary to optimise the existing axle design. So, a rectangular piece was suggested as the suitable design for the JD955 rear axle middle section.

Correspondence: Hassan Masoudi, Department of Biosystems Engineering, Faculty of Agriculture, Shahid Chamran University of Ahvaz, Iran.
Tel./Fax: +98.6133364057.
E-mail: hmasoudi@scu.ac.ir

Key words: cereal combine harvester, finite element analysis, modelling, optimisation, rear axle.

Acknowledgements: this work was supported by the vice chancellor for research and technology of Shahid Chamran University of Ahvaz, Iran [grant number 94/3/02/31579]. The authors thank the Shahid Chamran University of Ahvaz for this financial support.

Received: 21 May 2022.
Accepted: 12 October 2022.
Early view: 8 February 2023.

Journal of Agricultural Engineering 2023; LIV:1448
doi:10.4081/jae.2023.1448

Introduction

Applying new technologies to design agricultural vehicles and, as a result, their high reliability can prevent the fracture of machine parts and delays in sensitive to-time agricultural operations. A combine harvester is one of the cereals harvesting machines that work in complex, and uneven conditions. Many loads are applied to the combine in working conditions, so its parts must have enough resistance and be able to withstand the various loads. The axle is a shaft between two wheels, and its functions are: maintaining the position of wheels relative to each other and to the vehicle body, bearing the weight of the vehicle and external loads, absorbing shocks due to the road roughness, and resisting the applied bending moments and loads. The combine rear axle is most likely to be failed in uneven agricultural lands and costs the farmer both financially and in terms of time. In practice, the axle faces some stimulus, such as resonance, fatigue, and failure stresses. The fracture of the rear axle shaft occurs because of a momentary shock load or fabrication process defectives (Mujahidin and Andoko, 2019), and the main parts of the axle must be strong before any additional loading (Nanaware and Pable, 2003). Therefore, the type, position, and value of applying loads to the axle must be specified correctly for the optimal design of the axle. Meanwhile, the axle design process requires both static and dynamic analyses.

The strength of machine parts can be checked using finite element analysis (FEA) software to select the most suitable material (Pourdarbani and Tarighi, 2019). The FEA is a powerful method for determining the machine parts' stress, strain, and deformation under various loads. This method allows analysis in software environments without needing a physical model. So, the FEA can identify critical and non-critical points of machine parts quickly and confidently (Jahanbakhshi *et al.*, 2018). Modal analysis is the process of determining the dynamic parameters of a system, including the natural frequencies, damping coefficients, and shape of modes, to use them for creating a mathematical model of the system's dynamic behaviour. With the help of modern FEA, almost any linear dynamic structure can be discretised, and as a result, the capabilities and scope of theoretical modal analysis have been significantly increased (Ewins, 2000). A satisfactory correlation exists between design by analytical method and the FEA results (Dhande and Ulhe, 2014).

Various studies have been conducted on the design and analysis of agricultural vehicles parts by a computer during the last decades, such as ploughs (Jahanbakhshi *et al.*, 2018), tractors (Mahanty *et al.*, 2001; Rasekh *et al.*, 2009; Jahanbakhshi and Heidarbeigi, 2019), combine harvesters (Azadbakht *et al.*, 2013a; Azadbakht *et al.*, 2013b; Hussain *et al.*, 2022), sugarcane loader (Azevedo *et al.*, 2020), heavy-duty trucks (Leon *et al.*, 2000; Abd Rahman *et al.*, 2008; Topaç *et al.*, 2009; Avikal *et al.*, 2020; Tretjakovas and Čereška, 2021) and mini truck (Guo *et al*., 2020). Some researchers analysed the tractor-trolley axle using FEA (Paul *et al.*, 2013; Ramachandran *et al.*, 2016). When the trailer tank was full, the trailer axle static loads, shear forces, and bending moments were calculated. The results showed that the existing axle was essentially safe but was not ideal and needed to be modified. The maximum von Mises stress occurred at both ends of the existing and proposed shaft but in smaller areas with fewer values in the proposed shaft (Bansal and Kumar, 2012).

The tractor is the main machine in agriculture and is almost used in all operations, so its parts are under different loads and should be strong enough. Tarighi *et al.* (2011) performed a static and dynamic analysis of the front axle shell of the Mitsubishi MT 250D tractor by the FEA using SolidWorks and CosmosWorks, v. 2010 softwares. The values allowable stress and safety factors were less than the required values. In Oyyaravelu *et al.* (2012) study, the FEA was carried out on the front axle of a tractor using ANSYS software. The stress value exceeded the safe limit, and total deformation showed that the fracture was unavoidable. Modification of the axle geometry was suggested, and analysis was done with the same load and boundary conditions. The stress value and total deformation of the modified axle were within the safe limits. Aduloju *et al.* (2014) investigated the effect of angular displacement of the front axle of a tractor relative to its cast iron support shell to find the worst load conditions on the support using Pro-Engineer and MATLAB softwares. The failure analysis by Pro-Mechanica software showed that the safety factor was good. In Pourdarbani and Tarighi's (2019) study, the Cm45 steel was proposed to fabricate the front axle of the MF285 tractor based on the safety factor in static loading obtained from the FEA by ANSYS software.

Combine harvesters are the standard machines for farm product harvesting. Jafari *et al.* (2006) analysed the front axle of the JD955 combine harvester in static and dynamic loading to evaluate its mechanical strength using ANSYS v.9 software. The axle safety factor was very low and decreased under cyclic loading in field operations. Therefore, the use of a stronger body and reduced welding point were suggested for modification. Khanali *et al.* (2010) performed the FEA for the front axle of the JD955 combine harvester under static loading conditions. The calculated value of the safety factor was very low, so the front axle of this combine needed to be optimised. The results were proved using experimental methods too.

The main objective of this research was to determine the strength of the rear axle of JD955 combine harvester under real static and dynamic loads while moving on the road and farm. Finally, the optimal design of the axle was proposed to prevent axle fracture while working on the farm.

Materials and Methods

The rear axle specifications

JD955 combine harvester is the standard cereal harvesting machine in Iran. The rear axle of the JD955 combine harvester has been made from a thin-walled, hollow steel shaft with a uniform thickness of 8 mm (Figure 1). Each side of the axle is connected to the rim of the rear wheels by a spindle, and its middle part (pivot) is connected to the combine body through a kingpin. This axle is a dead shaft that bears only the combine weight and the wheels' loads and does not transmit any torque. The mechanical properties of the axle material are according to Table 1.

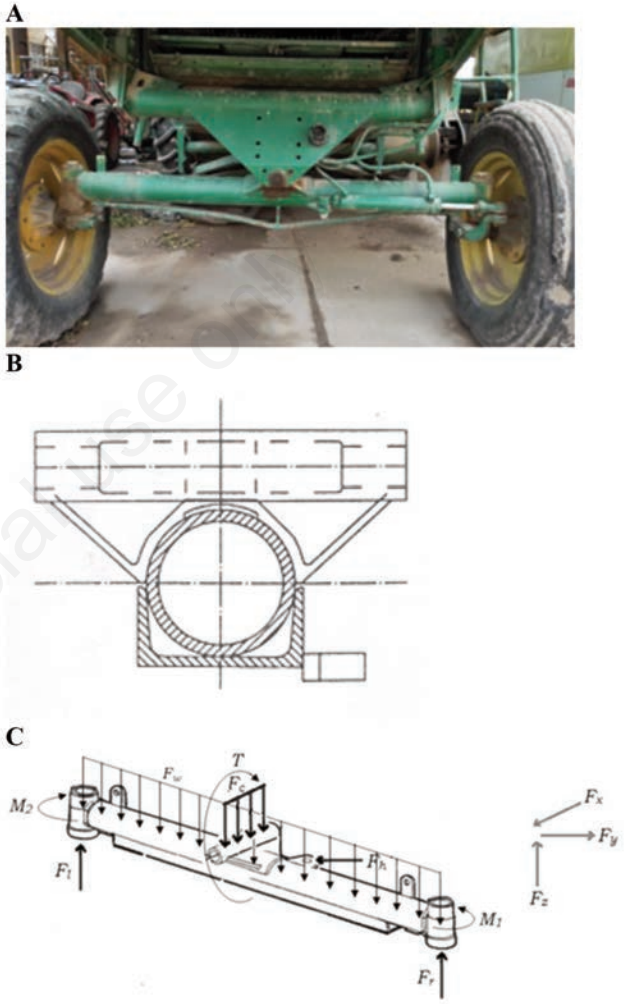

Figure 1. A) Rear axle of JD955 combine harvester; **B)** cross section of the axle; **C)** loads on the rear axle of combine harvester in static mode.

Table 1. Mechanical properties of the rear axle of JD955 combine harvester (Budynas and Nisbett, 2011).

Characteristic	Sign	Value
Material type	St	Construction steel
Density	ρ	7850 kg/m^3
Tensile strength	S_{ut}	460 MPa
Yield strength	S_y	250 MPa
Poisson's ratio	ν	0.3
Modulus of elasticity	E	207 GPa

The rear axle loads

According to Figure 1, loads applied to the rear axle of the combine in static mode are axle weight (F_W), steering cylinder force (F_h), rear wheels' reaction forces (F_r and F_l), and vertical load from the combine body (F_C). F_W has a constant value and is applied across the axle length. F_h can be measured by the hydraulic oil pressure of the steering system while the combine is moving. According to the combine catalogue, the weights on two rear wheels in static mode are 1610, 1290, and 1040 kg without the cutting platform when the platform is down and when the platform is up, respectively. F_C value changes when the combine moves in various operating conditions and must be measured.

Measuring the vertical load of the axle

An electronic force measurement system was fabricated to determine the real load on the middle of the axle (FC) (Rezaei *et al.*, 2022). The system consisted of a coupling, a compression load cell with10 tons capacity, an amplifying circuit for load cell output voltage, a data logger, and a laptop. The coupling consisted of two steel plates, one connected to the combine body via a kingpin and the second to the combine rear axle via another pin. The combine weight was transferred to the axle only through the load cell located in the middle of the coupling. The data logger received and saved load voltages from the load cell and transmitted them to the laptop for analysis.

Field tests were performed to determine the loads on the axle in working conditions at three locations, including dirt road, asphalt road, and wheat farm (Figure 2). The dynamic loads on the rear axle were determined, and the data from these tests were used for the next analysis.

Modelling and analysis of the axle

A 3D geometric model of the axle was designed in CATIA v.2015 software. All components were placed so that there was no movement between them. For the convenience of analysis, some components, such as spindles and hydraulic cylinders, were removed in the simplified model.

ANSYS Workbench v. 2015 was used for FEA, and desired parameters were obtained (Mokhtari *et al.*, 2015). Mechanical properties of the axle components were introduced to the software according to Table 1. The meshing of the model was done using the Solid95 element by considering the finest elements (at the model corners with 0.290740 mm length edges) to achieve more accurate results (Chaphalkar and Khetre, 2016). For applying boundary conditions, the two sides of the axle, which are the junctions of spindles, were introduced as fixed supports in the software. All wide loads were defined as compressive loads over the upper surface of the axle. The load cell forces were defined as concentrated loads on the lower half of the pinhole's inner surface. Finally, the amount of deformation, von Mises stress and strain, structural error (SE), fatigue life, and fatigue safety factor were determined for all loads applied to the axle in static, harmonic, transient, and dynamic analysis.

Theory of analysis

The modal analysis was used to find the axle's natural frequencies and the shape of natural modes. When a vehicle such as a combine harvester travels on a rough road, the frequency of loads on it is calculated from Eq. (1):

$$f = V/\lambda \quad (1)$$

where V is the vehicle velocity (m/s), λ is harmonic movement wavelength (m), and f is the applied frequency to the vehicle in motion (Hz). According to rows spacing in seed planters, 15 to 40 cm (Srivastava *et al.*, 1995), and the forward speed of combine harvesters on a farm (1.2 to 20 km/h) (Hunt, 2001), the maximum excitation frequency of the combine while working in a farm is obtained from Eq. (2):

Figure 2. Field tests in: **A**) asphalt road; **B**) dirt road; **C**) wheat farm.

$$f_{max} = 20/(3.6\times0.15) = 37.04\ \text{Hz} \quad (2)$$

So, to prevent resonance and early fracture of the axle, the first natural frequency of the axle should be more than twice the excitation frequency, *i.e.*, more than 75 Hz (Budynas and Nisbett, 2011).

The SE shows the amount of lost energy in loading; its unit is millijoules (mJ). By calculating this parameter, it is determined where the model meshing needs to be finer to have more accurate results-areas of the model with high errors in stress calculation identified by the SEs determination.

The combine rear axle was assumed to be a fixed-ended beam under harmonic and transient loads at its midpoint (Tarighi *et al.*, 2011). Completely inverted oscillating loads were applied to the axle according to its natural frequencies for harmonic analysis. The transient analysis was done in two stages. First, the maximum transient force (F_{max}) was considered to be six times the static load (Khanali *et al.*, 2010). In dynamic analysis, from the data recorded in field tests, the effects of 20 loads on the axle were investigated throughout 20s for each path.

Results and Discussion

The average values of maximum loads applied to the combine rear axle in various working conditions are shown in Figure 3. For example, minimum and maximum loads were obtained equal to 15.067 KN and 49.167 KN in stopped mode and moving uphill a dirt road, respectively. The real loads were defined as concentrated forces applied to the middle of the axle in all analyses.

In the modal analysis, the axle's values of six natural frequencies were obtained from 11.86 to 216.91 Hz, as shown in Table 2. These frequencies were used to apply harmonic loads. Since the axle deformations may not be acceptable for all frequencies, deformation at each frequency was determined separately to identify at which frequency the deformation is more uniform and logical. Then, the harmonic analysis was performed for that frequency.

According to Table 2, most natural frequency modes of the JD955 combine harvester are more than 75 Hz, except for the first natural frequency, so no resonance occurs at these frequencies. However, in the first frequency, there is a possibility of resonance phenomenon during the combine movement inside a farm, and it is better to change the axle structure.

Axle deformations

Table 3 shows the total deformations of the axle in maximum load for various analyses. A relatively linear relationship exists between the deformation value and the amount of the applied load. The least deformation occurred for the most minor loads, *i.e.*, 15.067 KN in static loading at the workshop. However, the maximum deformation occurred in 18.830 KN and 49.167 KN loads, respectively. Maximum directional deformation occurred in Z-axis direction (perpendicular to the loading direction), which caused a slight bending in the middle of the lower connection of the axle in the +Z direction.

Two samples of the axle deformation in static and harmonic analysis are shown in Figure 4. By performing a modal analysis dependent on static analysis, the frequency deformations of the axle were obtained more realistically. The most and the least deformation along X-axis occurred symmetrically on both sides of the lower part. However, in general,, the highest deformation occurred in the middle of the lower part, and the least deformation occurred in the spindles at both ends of the axle. In harmonic analysis, the axle deformation had an inverted linear ratio with the load value, and the values were generally very small in all directions. Changes in Y and Z directions were very few, and most occurred in the X axis.

Figure 5 shows two samples of velocity and acceleration of the axle deformations in transient analysis. The axle's total deformation happened with more velocity and acceleration in its middle section, which is actually the axle's gravity centre. In dynamic analysis, although there was a linear relationship between the load and deformation in each direction, the deformations had fewer values than static and transient analysis and more than harmonic analysis.

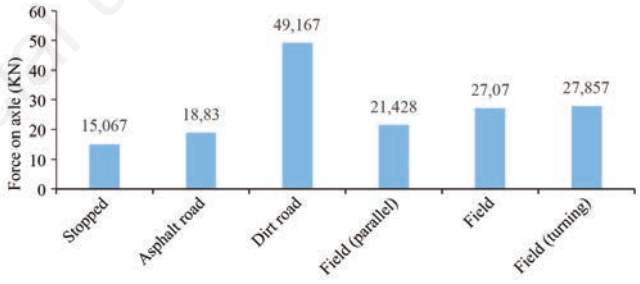

Figure 3. Average values of maximum loads on the combine rear axle in various working conditions.

Table 2. Six first natural frequencies of the axle.

Vibrating mode	Vibrating frequency (Hz)
1	11.86
2	100.19
3	144.79
4	165.75
5	178.19
6	216.91

Table 3. The total deformations of the axle in various analyses (mm).

Test conditions	Maximum load (KN)	Static analysis	Harmonic analysis	Transient analysis
Stationary mode	15.067	0.089-1.038	2.5^{-15}-5.3^{-13}	0.031-0.660
Asphalt road	18.830	0.110-1.293	2.3^{-15}-4.8^{-13}	0-0.303
Dirt road	49.167	0-1.280	0-1.55^{-16}	0.031-0.683
Parallel to furrows	21.428	0-0.561	0-6.77^{-17}	0-0.385
Perpendicular to furrows	27.075	0-0.707	0-8.55^{-17}	0-0.389
Farm end turning	27.875	0-0.726	1.1^{-19}-5.2^{-16}	0-0.389

The combine's rear axle is a solid steel structure and showed elastic behaviour against the loads. In fact, the deformations created in it, although very small, were elastic. Since the axle behaviour against loads never exceeded the elastic limit, its deformations were proportional to the applied forces in most analyses. Therefore, Hooke's law, which represents the linear relationship between force and deformation, was established for the axle. So, equations related to elastic structures could be used to calculate stress and strain in the axle.

Von Mises stress and strain

Von Mises stress and strain distributions throughout the axle structure were very similar in all analyses. According to Table 4, maximum von Mises stress and strain in the axle were obtained due to static, transient, dynamic, and harmonic loading, respectively.

In harmonic analysis, von Mises' maximum stress and strain occurred in some points of the lower part at its middle and near the spindles. Average values of these parameters occurred at scattered points of the lower part and junction points of the spindles and

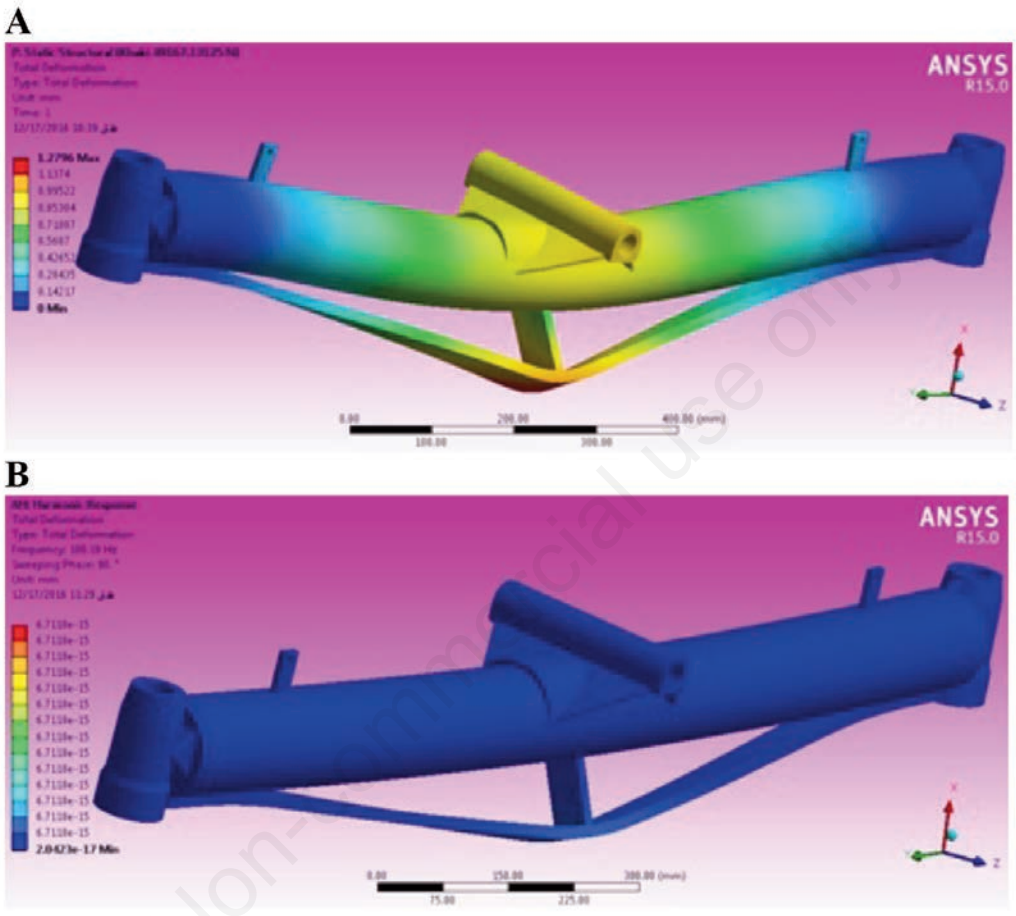

Figure 4. A) Total deformation of the axle in the static analysis under 49.167 KN loading; **B**) total deformation of the axle in harmonic analysis at a frequency of 100.19 Hz.

Table 4. Range of the axle von Mises stress and strain values in various analyses.

	Load (KN)	Static analysis	Harmonic analysis	Transient analysis
Stress	15.067	0.0008-115.76	2.373^{-16}-3.680^{-11}	0.00058-83.784
	18.830	0.0011-143.87	2.132^{-16}-3.32^{-11}	0.00065-401.05
	49.167	0.0018-1200	1.0095^{-9}-1.74^{-14}	0.00062-85.848
	21.428	0.0011-527.52	4.399^{-20}-7.604^{15}	0.00107-489.17
	27.075	0.0013-619.54	5.549^{-20}-8.874^{-15}	0.00109-494.17
	27.875	0.0012-636.54	2.009^{-19}-6.077^{-14}	0.00109-486.66
Strain	15.067	9.50^{-9}-0.00078	3.17^{-21}-2.323^{-16}	9.439^{-9}-0.00042
	18.830	1.18^{-9}-0.00097	2.853^{-21}-2.094^{-16}	5.814^{-9}-0.00205
	49.167	2.37^{-8}-0.0062	5.81^{-25}-8.942^{-20}	9.637^{-9}-0.00043
	21.428	1.03^{-8}-0.0027	2.533^{-25}-3.897^{-20}	9.146^{-9}-0.0029
	27.075	1.28^{-8}-0.0037	2.211^{-25}-5.328^{-20}	9.311^{-9}-0.0029
	27.875	1.29^{-8}-0.0038	1.917^{-24}-3.080^{-19}	9.332^{-9}-0.0029

main shaft. Other axle areas, including the triangular shape part, the main shaft, and the spindles, had the least stress and strain values. In transient analysis, the highest values of von Mises stress and strain occurred in the middle of the lower part, and the least values occurred in the spindles and some points of the kingpin hole (Figure 6). Dynamic analysis showed that the axle loads were not very much in the form of impact loads. However, they are a bunch of near-value loads that enter the axle for a while. So, the dynamic analysis stresses, strains, and deformations were less than other analyses. Strain changes in the static and harmonic analysis were very different. While the axle strain changes in the dynamic analysis were very similar to the static analysis.

Structural error

The axle SE values were close to zero, so calculated stress values were relatively accurate. The distribution of SE was almost the same in all loadings, and most of the axle areas had no problem showing the stress parameter. But, two ends and the middle of the lower part, some points between the main shaft and the triangular shape part, and a few points between the main shaft and spindles had very low SE values. Maximum values of the axle SE in the static and transient analysis are shown in Table 5. The maximum SE occurred at the highest concentrated load, *i.e.*, 49.167 KN. So, the more applied, the more accurate meshing. Maximum SE had a minimal increase with the load increasing like deformation.

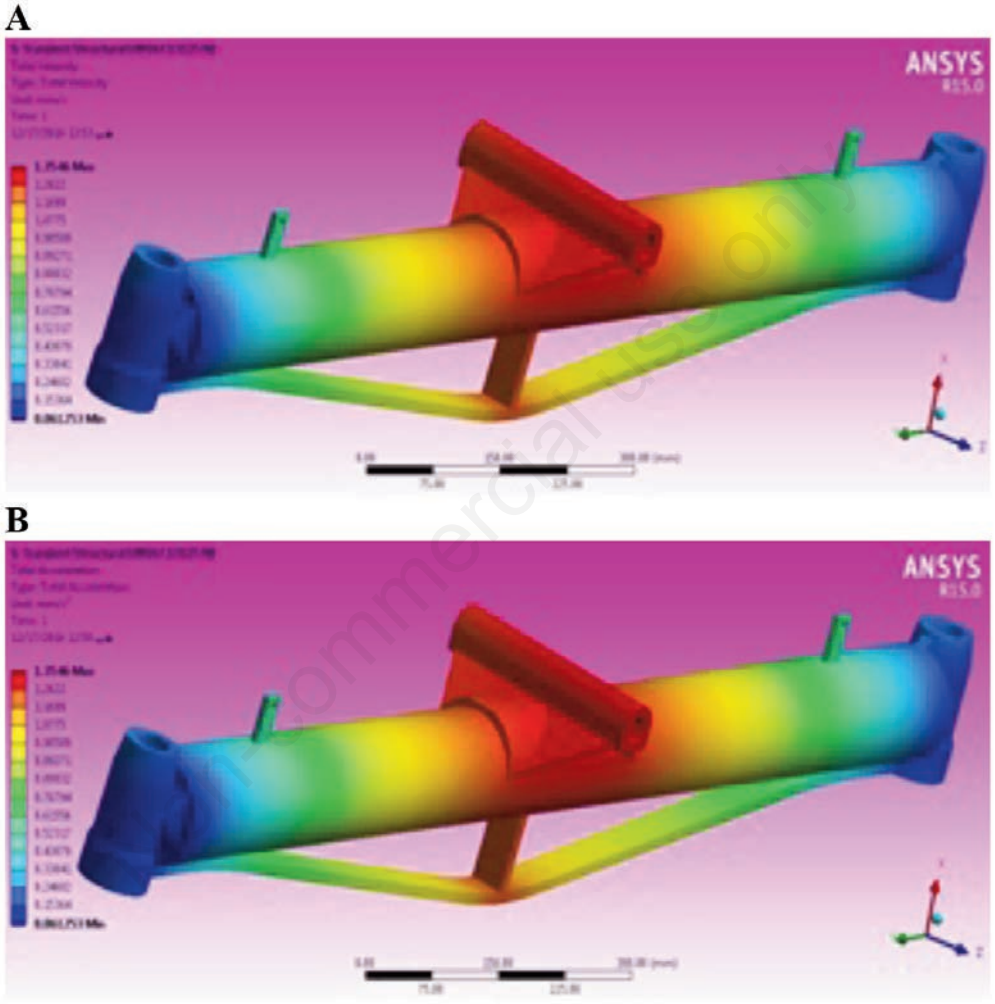

Figure 5. **A**) Total velocity (mm/s); **B**) total acceleration (mm/s^2) of the axle in transient analysis.

Table 5. Maximum standard error in the static and transient analysis under concentrated loads.

Test conditions	Maximum load (KN)	Static analysis (mJ)	Transient analysis (mJ)
Stationary mode	15.067	2.2962	2.2962
Asphalt road	18.830	17.942	1.666
Dirt road	49.167	21.72	2.409
Parallel to furrows	21.428	4.196	2.688
Perpendicular to furrows	27.075	6.657	2.743
Farm end Turning	27.875	7.034	2.743

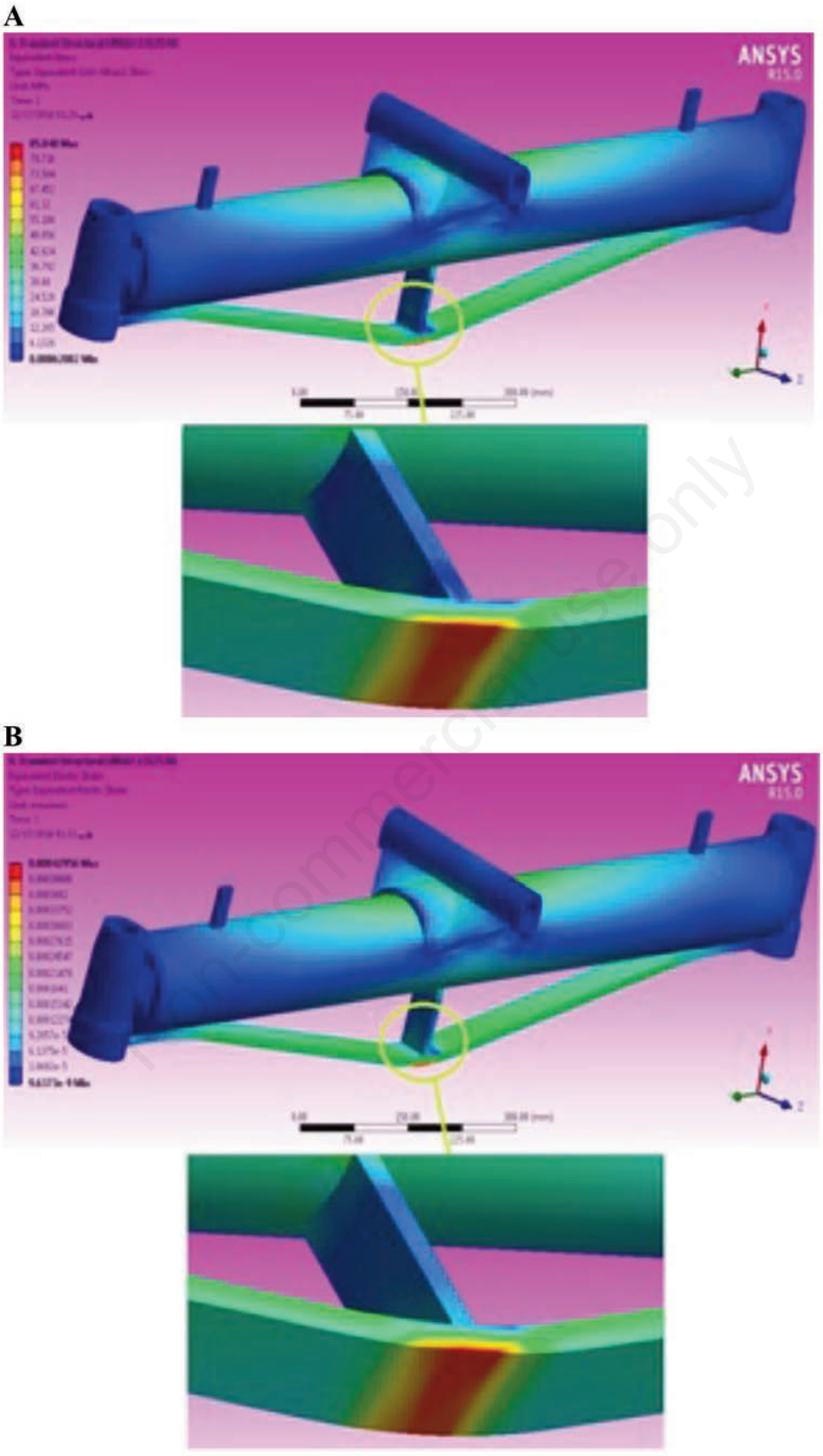

Figure 6. **A**) Von Mises stress; **B**) von Mises strain under a load of 49.167 KN in transient analysis.

Nevertheless, the minimum SEs fluctuated with the load increasing. In total, most axle areas had low SE, and the axle meshing was correct and acceptable.

Fatigue life

The whole axle was defined as one piece, and its working life was obtained at each loading (Figure 7). The axle fatigue life for most of the loads was more than 10^6 cycles, but at high loads, some points of the axle had a shorter life. As shown in Table 6, in the static analysis, the less fatigue life was for 49.167 KN loading, obtained when the combine moved uphill of dirt road. In transient analysis, less fatigue life was obtained under a load of 27.075 KN, obtained when the combine moved perpendicular to furrows inside the farm.

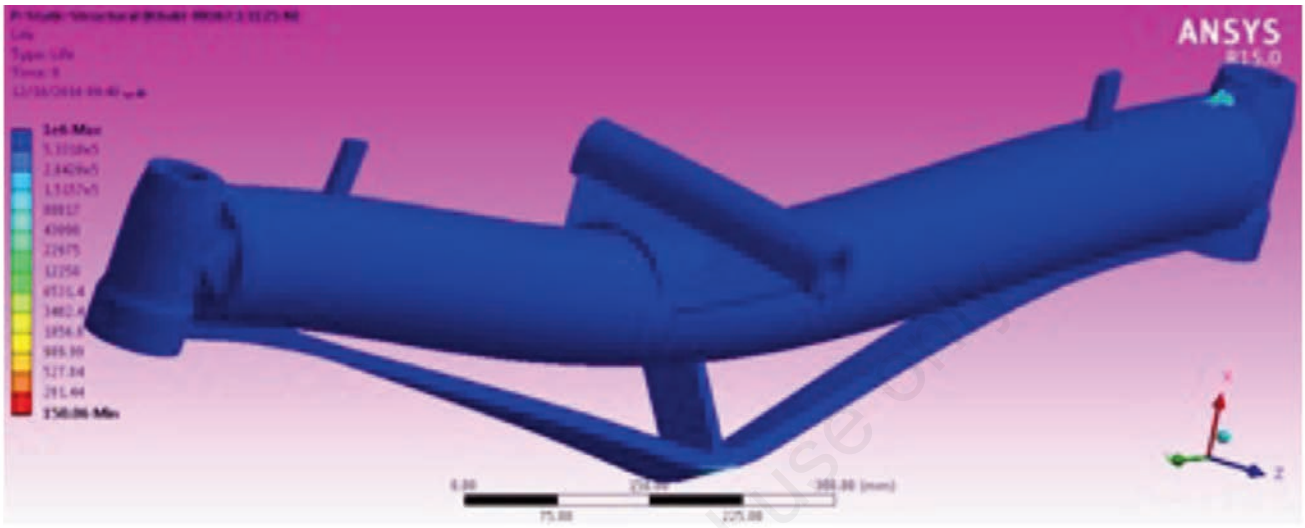

Figure 7. The axle fatigue life under the load of 49.167 KN.

Table 6. The axle fatigue life ranges in static and transient analysis (cycle).

Test conditions	Maximum load (KN)	Static analysis	Transient analysis
Stationary mode	15.067	1.892e5-10^6	1000000
Asphalt road	18.830	85838-10^6	2682.3-10^6
Dirt road	49.167	150.06-10^6	1000000
Parallel to furrows	21.428	1255.2-10^6	1527.4-10^6
Perpendicular to furrows	27.075	826.26-10^6	1487.5-10^6
Farm end turning	27.875	770.1-10^6	1547.9-10^6

Table 7. Range of the axle fatigue factor of safety in static and transient analysis.

Test conditions	Maximum load (KN)	Static analysis	Transient analysis
Stationary mode	15.067	0.745–15	1.029–15
Asphalt road	18.830	0.599–15	0.215–15
Dirt road	49.167	0.072–15	1.004–15
Parallel to furrows	21.428	0.163–15	0.176–15
Perpendicular to furrows	27.075	0.139–15	0.174–15
Farm end Turning	27.875	0.135–15	0.177–15

Table 8. Various parameters for the proposed design of axle in different loads.

Test conditions	Static analysis	Transient analysis	Harmonic analysis
Total deformation (mm)	0.253-1.976	0.0402-1.964	1.342^{-17}-4.54^{-16}
von Mises stress (MPa)	0.0024-263	0.0015-264.6	1.524^{-18}-2.735^{-13}
von Mises strain	2.716^{-8}-0.00172	3.072^{-8}-0.0013	1.12^{-23}-1.451^{-18}
Fatigue factor of safety	0.328-15	0.326-15	-

The fatigue factor of safety

Two samples for the factor of safety distribution along the axle are shown in Figure 8. More axle points had a safety factor of less than 15, the maximum safety factor in the software. Some points of the kingpin hole, the triangular shape part wings, most of the main shaft surface, most of the lower part areas, and some points between the main shaft and the spindles had a safety factor of less than 15. However, areas of the spindles that were opposite to the main shaft junction, two ends of the kingpin hole, had a safety factor equal to 15.

The range of the fatigue factor of safety due to concentrated loads in the static and transient analysis is shown in Table 7. In the static analysis, by increasing the load, unsafe areas gradually increased, and areas with a safety factor equal to 15 decreased. The areas close to the spindles, the middle of the main shaft, and the middle of the lower part had the least safety factor, equal to 0.072 for 49.167 KN loading. In the transient analysis, the safety factor values for unsafe areas were between 1.82 and 10, and very few points were faced with the least safety factor. Moreover, the minimum safety factor was equal to 1.004 for 49.167 KN loading.

Proposed design for the axle

According to the results of various analyses, optimisation of the existing design of the JD955 combine harvester axle was necessary; therefore, two designs were proposed as follows:

a) Thickness of two edges of the triangular shape part that are welded to the main shaft and the kingpin hole be increased by about 10 mm, and the thickness of the other two edges be increased by about 2 to 5 mm.
b) Wings of the triangular shape part be removed and replaced with cubes because a rectangular mass balance is better than a triangular mass balance and can keep the axle balanced in the ups and downs of a moving path. It will also have better stress resistance.

To ensure the effectiveness of these two plans, both were designed in CATIA software and transferred to ANSYS Workbench software. Then the same analysis- previously performed for the existing axle- was done with the maximum measured load, *i.e.*, 49.167 KN. Results of the analysis showed that both plans were more robust than the existing design, but the superiority of the second design was quite evident. Therefore, Figure 9 was proposed as a suitable design for the rear axle of the JD955 combine harvester. As shown in Table 8, von Mises's stress and

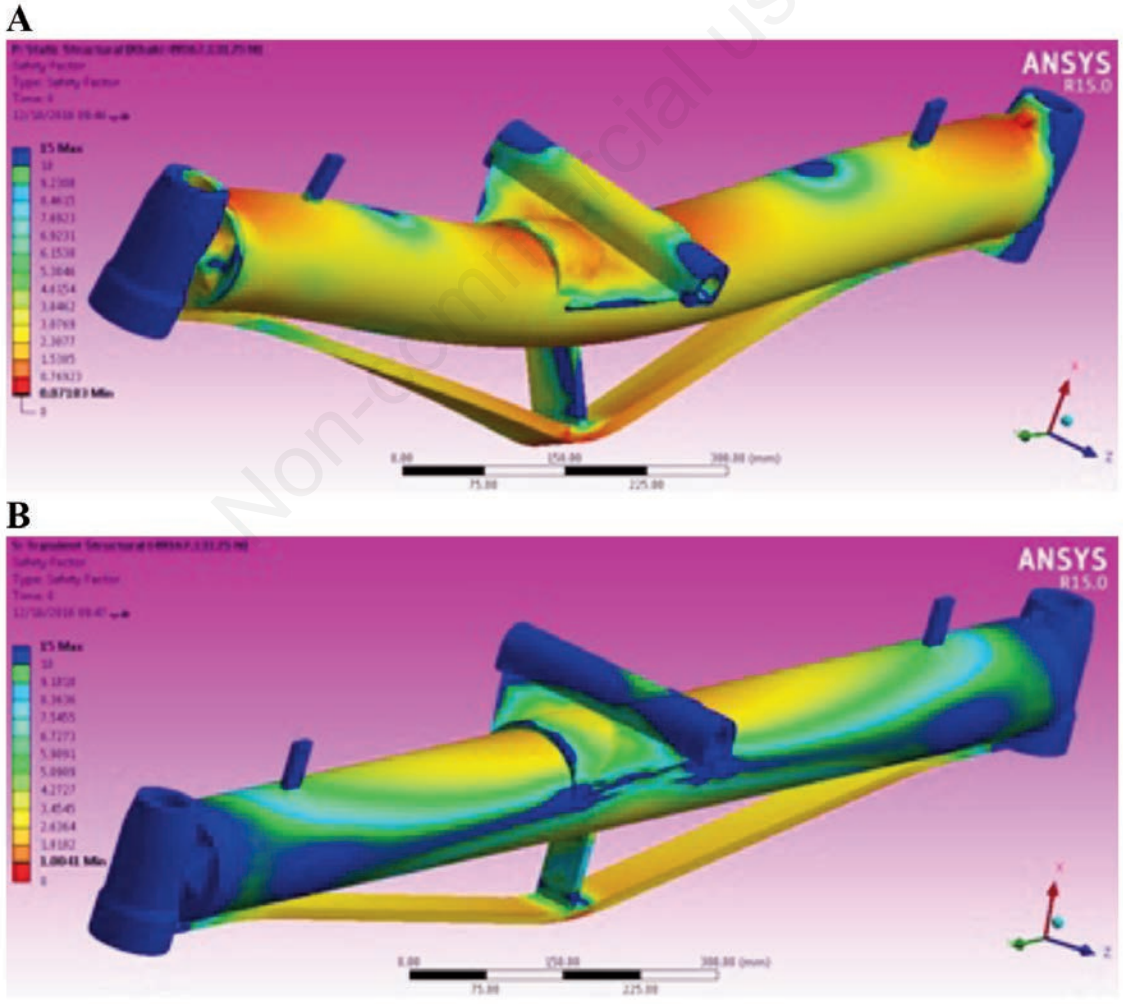

Figure 8. Distribution of the fatigue factor of safety along the axle under a load of 49.167 KN in **A**) static and **B**) transient analysis.

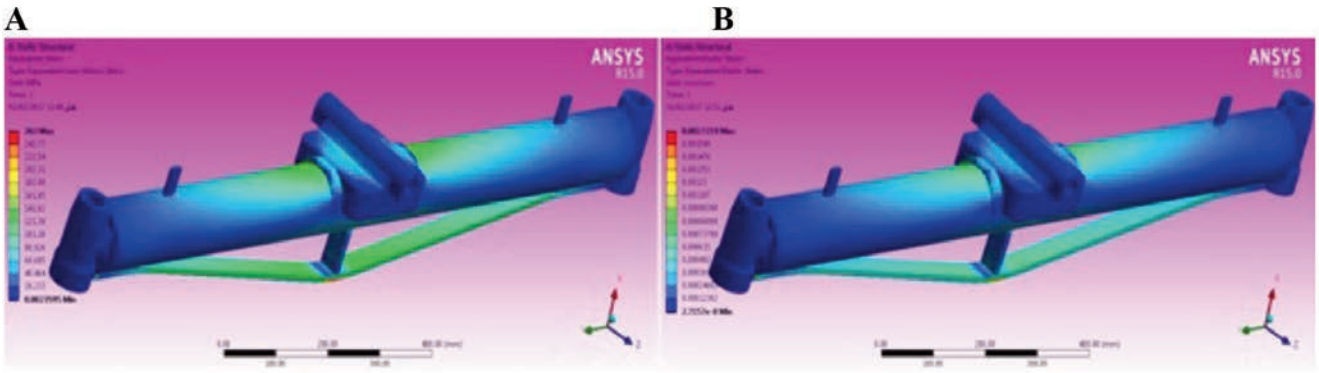

Figure 9. Static analysis of the proposed axle; **A**) von Mises stress; **B**) von Mises strain.

strain values for the proposed axle were approximately a quarter of the same values for the existing axle. Also, the safety values for static and transient loading were much more and almost eight times compared to the existing axle.

Some samples for static analysis of the proposed axle are shown in Figure 9. Although total deformations or the proposed axle in various loads were slightly more than values obtained for the existing axle, much less bending occurred in the middle of the axle. Using more resistance material can cover this slight deformation. High von Mises stress areas were reduced in the proposed design. The distribution of safety factors in the proposed design was almost similar to the existing design, but areas with low safety factors were smaller.

Conclusions

From real-time data collection, it was found that most loads applied to the middle of the rear axle of the JD955 combine harvester were between 10 and 20 KN. When climbing an uphill, the maximum unusual load applied to the axle was about 50 KN. The results of this maximum load were used to optimise the existing design of the JD955 rear axle. The existing rear axle of the JD955 combine harvester was subject to much stress at some very uneven ups and downs, which may be fractured over a long time. If the axle joint points to the spindles (which are axle supports) and the axle middle part (which is the axle centre of gravity) are strengthened, less deformation and low stress and strain will occur in the axle and its safety factor will increase. Finally, in order to optimise and increase the strength and reliability of the rear axle of the JD955 combine harvester, the following changes were suggested:

- Using a rectangular piece instead of the triangular shape part in the middle of the axle;
- ncreasing thickness of the triangular shape part in the middle of the axle;
- Using a stronger alloy for the middle of the axle, especially for the triangular shape part.

Nomenclature

λ: harmonic movement wavelength (m)
ν: Poisson's ratio
ρ: density
E: modulus of elasticity
f: applied frequency to the vehicle in motion (Hz)
f_{max}: maximum excitation frequency
F_C: vertical load from combine body
F_h: steering cylinder force
F_{max}: maximum transient force
F_r and Fl: rear wheels' reaction forces
F_W: axle weight
S_{ut}: tensile strength
S_y: yield strength
V: vehicle velocity (m/s)
FEA: finite element analysis
SE: structural error
St: steel

References

Abd Rahman R., Nasir Tamin M., Kurdi O. 2008. Stress analysis of heavy duty truck chassis as a preliminary data for its fatigue life prediction using FEM. J. Mek. 26:76-85.

Aduloju S.C., Mgbemena C.O., Ebhota W.S., Bolarinwa G.O. 2014. Computer aided structural analysis of axle tilting effect on tractor front axle support. Innov. Syst. Des. Eng. 5:12-31.

Avikal Sh., Bisht A., Sharma D., Hindwan H., Yadav S., Kumar K.C.N., Thakur P. 2020. Design and fatigue analysis of front axle beam of a heavy duty truck using ansys. Mat. Today: Proc. 26:3211-5.

Azadbakht M., Esmaili Shayan M., Jafari H. 2013a. Investigation of long shaft failure in John Deere 955 grain combine harvester under static load. Univers. J. Agric. Res. 1:70-3.

Azadbakht M., Taghizadeh-Alisaraei A., Hashemi A., Janzadeh Galogah R. 2013b. Analysis of stresses on straw walker crankshaft of John Deere 995 combine harvester. Univers. J. Agric. Res. 1:9-16.

Azevedo T.F., Sampaio W.R.V., Câmara E.C.B., Lima G.D., Silva W.F.S., Ramos S.S. 2020. Failure analysis of a sugarcane loader rear shaft. Eng. Fail. Anal. 109:104326.

Bansal H., Kumar S. 2012. Weight reduction and analysis of trolley axle using ANSYS. Int. J. Eng. Manag. Res. 2:32-6.

Budynas R.G., Nisbett J.K. 2011. Shigley's mechanical engineering design. 9th ed. Series in Mechanical Engineering; McGraw-Hill, New York, NY, USA.

Chaphalkar S.P., Khetre S. 2016. Design and model analysis of rear axle with two ends spur geared using FEA. Int. J. Mech.

Eng. Tech. 7:502-9.
Dhande K.V., Ulhe P. 2014. Design and analysis of front axle of heavy commercial vehicle. Int. J. Sci. Tech. Manag. 3:114-22.
Ewins, D.J. 2000. Modal testing: theory, practice and application. 2nd ed. Research Studies Press Ltd., Hertfordshire, UK.
Guo W., Ding N., Xu N., Liu L., Li N., Shi J., Wu C.L. 2020. Fracture analysis of a welded front axle tube structure from a mini-truck. J. Mech. Sci. Technol. 34:109-16.
Hunt D.R. 2001. Farm power and machinery management, laboratory manual and work. Translated by M. Behroozi-Lar. Tehran University Press, Tehran, Iran [In Farsi].
Hussain S., Zheng D., Song H., Farid M.U., Ghafoor A., Ba X., Wang H., Wang W., Sher A., Alshamali S.J. 2022. Computational fluid dynamics simulation and optimisation of the threshing unit of buckwheat thresher for effective cleaning of the cleaning chamber. J. Agric. Eng. 53:1230.
Jafari A., Khanali M., Mobli H., Rajabipour A. 2006. Stress analysis of front axle of JD955 combine Harvester under Static Loading. J. Agric. Soc. Sci. 2:133-5.
Jahanbakhshi A., Heidari Raz Darreh S., Kheiralipour K. 2018. Simulation and static and fatigue analysis of cross bar of moldboard plough by finite element method (FEM). Iran J. Biosyst. Eng. 49:341-52. [In Farsi].
Jahanbakhshi A., Heidarbeigi K. 2019. Simulation and mechanical stress analysis of the lower link arm of a tractor using finite element method. J. Fail. Anal. Preven. 19:1666-72.
Khanali M., Jafari A., Mobli H., Rajabipour A. 2010. Analysis and design optimization of a frontal combine harvester axle using finite element and experimental methods. J. Food Agric. Environ. 8:359-64.
Leon N., Martinez P.O., Adaya P. 2000. Reducing the weight of a frontal axle beam using experimental test procedures to fine tune FEA. In 2nd Worldwide MSC Automotive Conference, Dearborn, MI, USA.
Mahanty K.D., Manohar V., Khomane B.S., Nayak S. 2001. Analysis and weight reduction of a tractor's front axle. Tata Consultancy Services. Swarup Udgata, International Auto Limited, India.
Mokhtari A., Moradi M., Tarkesh Esfahani R. 2015. Modelling and analysis in ANSYS Workbench for Engineers; 2nd Press. Andishe Sara Publication, Tehran, Iran [In Farsi].
Mujahidin F., Andoko. 2019. Stress analysis of rear axle pick-up with finite element method. IOP Conf. Ser. Mater. Sci. Eng. 494:012028.
Nanaware G.K., Pable M.J. 2003. Failures of rear axle shafts of 575 DI tractors. Eng. Fail. Anal. 10:719-24.
Oyyaravelu R., Annamalai K., Senthil Kumar M., Naiju C.D., Michael J. 2012. Design and analysis of front axle for two wheel drive tractor. Adv. Mater. Res. 488:1808-12.
Paul I.D., Bhole G.P., Chaudhari J.R. 2013. Optimization of tractor trolley axle for reducing the weight and cost using finite element method. J. Eng. Comput. Appl. Sci. (JEC&AS) 2:31-5.
Pourdarbani R., Tarighi J. 2019. Choosing the proper material to optimize the front axle of the tractor Mf285 using finite element. Emir. J. Eng. Res. 24:Article 1.
Ramachendran, Paramesh G., Madhusudhan. 2016. Optimization of tractor trolley axle using FEM. Int. Refereed J. Eng. Sci. (IRJES) 5:52-61.
Rasekh M., Asadi M.R., Jafari A., Kheiralipour K. 2009. Obtaining maximum stresses in different parts of tractor (Mf-285) connecting rods using finite element method. Aust. J. Basic Appl. Sci. 3:1438-49.
Rezaei A., Masoudi H., Zaki Dizaji H., Khorasani Ferdavani M.E. 2022. Development of an electronic system for determining vertical loads on the rear axle of cereal combine harvesters in motion. J. Agri. Mach. 12:241-52.
Srivastava A.K., Goering C.E., Rohrbach R.P. 1995. Engineering principles of agricultural machines. Published by ASAE.
Tarighi J., Mohtasebi S.S., Alimardani R. 2011. Static and dynamic analysis of front axle housing of tractor using finite element methods. Aust. J. Agric. Eng. (AJAE) 2:45-9.
Topaç M.M., Günal H., Kuralay N.S. 2009. Fatigue failure prediction of a rear axle housing prototype by using finite element analysis. Eng. Fail. Anal. 16:1474-82.
Tretjakovas J., Čereška A. 2021. The truck trailer suspension axles failure analysis and modelling. Transport. 36:213-20.